GEOPHYSICAL RESEARCH LETTERS, VOL. 15, NO. 9, PAGES 1033-1036, AUGUST SUPPLEMENT 1988

PERMEABILITY OF ROCK SAMPLES FROM CAJON PASS, CALIFORNIA

C. Morrow and J. Byerlee

U.S. Geological Survey, Menlo Park, CA

Abstract. Room temperature, steady-state flow measurements of permeability were conducted on 15 unfractured core samples collected at depths between 270 and 2100 m in the Cajon Pass drillhole. Confining and pore pressures were set to the lithostat and hydrostat for each depth. The first 500 m encountered in the drill hole is composed of sandstones with typically high permeabilities of around $10^{-17} m^2$. The crystalline rocks between 500 and 2100 m show a systematic decrease in permeability with depth from 10^{-19} to less than $10^{-21} m^2$. These values are particularly low relative to the applied effective stresses of only 10-30 MPa, and may be a result of the extensive crack healing that was observed in most samples.

Introduction

The DOSECC drillhole at Cajon Pass, California, provides the unique opportunity to resolve some of the long-standing questions regarding the state of stress along the San Andreas fault. Observations of heat flow in shallow boreholes near the fault show no evidence of frictionally generated heat, implying that the average shear stresses acting on the fault are low. In contrast, frictional faulting theory and laboratory studies predict much higher stress levels. These stress constraints have been much debated in the literature (see for instance Lachenbruch and Sass, 1980; Brace and Kohlstedt, 1980).

Permeability is one of the physical properties of the fault zone rocks that is important to the interpretation of both heat flow and in situ measurements. This property quantifies the ease with which fluids can circulate through the fault gouge and surrounding rock. Permeability will influence the extent to which frictionally generated heat is transported by groundwater (O'Neil and Hanks, 1980), thereby obscuring the heat flow anomaly. It is also a major factor in the creation/relief of excess fluid pressures that may develop in the fault zone, altering the true effective stress acting on the rocks. Because many aspects of fault behavior are related to permeability, permeability measurements were conducted on core samples extracted during the first phase of the drilling program at Cajon Pass.

Sample Description

After the first phase of the program was completed, the hole had been drilled to a depth of 2100 m. The top 500 m consisted of arkosic sandstone, and the rest was a complex assemblage of crystalline rocks. Specimens from fifteen unfractured regions along the length of the core were chosen for study. Descriptive information on core number and section, rock type, depth, and orientation is given in Table 1. The two shallowest specimens were taken from the sandstone layer, and were selected for their contrasting textures. The specimen at 272 m was fine grained (<0.5 mm) and well sorted, whereas the specimen at 480 m contained lithic fragments up to 3 mm in diameter and was extremely friable. The deeper crystalline rocks were quite wide ranging in character, as Table 1 indicates, including granites, granodiorites, diorites and strongly foliated gneisses. Most have an average grain size of around 1 mm.

The sandstones were both cored in a horizontal direction along the reference azimuth line, which we have called 0° in this paper. The crystalline rocks were sampled in three orthogonal directions (vertical, 0°, and 90° to the azimuth line) in order to test for permeability anisotropy. The reference azimuth line is drawn when the core is removed, and must later be oriented relative to true north (Pezard et al., 1987). As a result, the horizontal directions vary widely from rock to rock.

Procedure

The samples from each depth were machined into test cylinders 2.54 cm in diameter and 2.54 cm long. These specimens were placed in the sample assembly as shown in Figure 1. The rock was sandwiched between stainless steel mesh shims, which allowed uniform flow of water into and out of the ends. (The steel spacers on either side of the shims were required only for the geometric constraints of the sample assembly.) This column was then jacketed in polyurethane tubing and sealed with wire clamps on the outside. Confining pressure (supplied by kerosene) was held constant by a computer controlled servo-mechanism. Pore pressure (deionized water) was held constant by a large volume reservoir on the outlet side of the sample. A pressure intensifier on the inlet side maintained the pressure differences across the sample at 1.0 MPa. The flow rate of water through the rock was determined by recording the change in volume of the intensifier with time. Temperature was maintained at 27° ± 0.5° in the experimental chamber in order to assure accurate pore fluid volume measurements. Permeability was measured over a period of 24 hours in each sample to establish steady-state flow. Values of permeability were calculated using Darcy's Law for fluid flow:

$$k = \frac{q\mu}{A} \left(\frac{dp}{dx}\right)^{-1} \quad (1)$$

Paper number 8L7328.

TABLE 1. Experimental Results

Core/Segment	Depth	Direction	Rock Type	P_c	P_p	P_e	$k(10^{-21}m^2)$
1/2	272.5 m	0 deg.	arkosic sandstone	6.1 MPa	2.7 MPa	3.4 MPa	54000
4/3	480.9	0	lithic arkosic sandstone	10.8	4.7	6.1	832.9
10/3	745.0	Vertical		17.5	7.3	10.2	208.7
	"	0 (27N)	granite				601.2 cracked
	"	90					217.1
13/5	1021.7	V	granodiorite	24.6	10.0	14.6	80.9
	"	0 (265N)					86.0
	"	90					74.7
15/3	1139.3	V	granodiorite	27.6	11.2	16.4	16.3
	"	0 (355N)					76.8
	"	90					59.7
16/3	1284.4	V	quartzose	31.4	12.6	18.8	1.0
	"	0 (040N)	gneiss				1.9
	"	90					1.9
17/6	1353.0	V	granodiorite	33.2	13.3	19.9	7.3
	"	0 (200N)					8.6
	"	90					24.5
19/4	1654.7	V	hornblende	41.2	16.2	25.0	5.8
	"	0 (087N)	granodiorite				10.6
	"	90	gneiss				12.1
20/3	1741.0	V		43.5	17.1	26.4	6.9
	"	0 (135N)	diorite				0.9
	"	90					4.0
26/5	1903.5	V	biotite	47.7	18.7	29.0	2.4
	"	0	hornblende				16.4 cracked
	"	90	gneiss				75.1 cracked
28/2	1983.3	V		49.8	19.5	30.3	4.1
	"	0	granodiorite				6.8
	"	90	gneiss				103.1 cracked
30/4	2042.3	V		51.3	20.0	31.3	1.5
	"	0	diorite				8.5
	"	90					2.0
31/4	2056.4	0	granodiorite	51.7	20.2	31.3	189.5
	"	90					107.7
33/4	2077.5	V	diorite	52.3	20.4	31.9	2.5
	"	0					1.9
	"	90					2.4
34/2	2113.5	V	hornblende	53.2	20.7	32.5	7.3
	"	0	diorite				6.3
	"	90					3.7

where q is the flow rate, A is the cross-sectional area of the sample normal to the direction of flow, μ is the dynamic viscosity of water (taken to be 1.0 cp in these experiments), and dp/dx is the fluid-pressure gradient. Steady-state measurements of very low permeabilities are possible with this system because of the small volume of the inlet reservoir (0.211 ml), which enables accurate pore fluid volume measurements with time.

The experiments were all run at the in situ confining and pore pressures encountered by the samples at depth. Confining pressures were based on the density log of the drill hole averaged every 100 feet, and pore pressures were calculated assuming a normal hydrostatic gradient. Many of the permeability measurements were conducted several times to test the repeatability of the system. In addition, the system was checked for leaks by monitoring the "flow" through an impermeable plug.

Permeability Results

Permeability values for the 40 samples are listed in Table 1. Permeability is given in m^2, (1 Darcy = 0.987 x $10^{-12}m^2$.) Because there were numerous joints, cracks, and filled fractures along the length of the core that were avoided during sampling, the measured permeabilities represent minimum rather than average values. A few samples, however, contained hairline fractures that resulted in abnormally high values. These rocks are indicated in the Table. Note that since the effective pressures, (P_c-P_p), vary with depth, a direct comparison of permeability values of different rocks would not be meaningful.

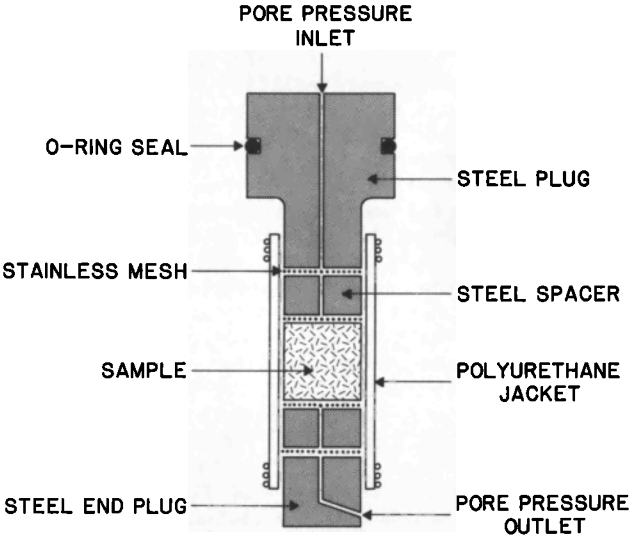

Figure 1. Experimental assembly for steady-state flow through a cylindrical rock sample.

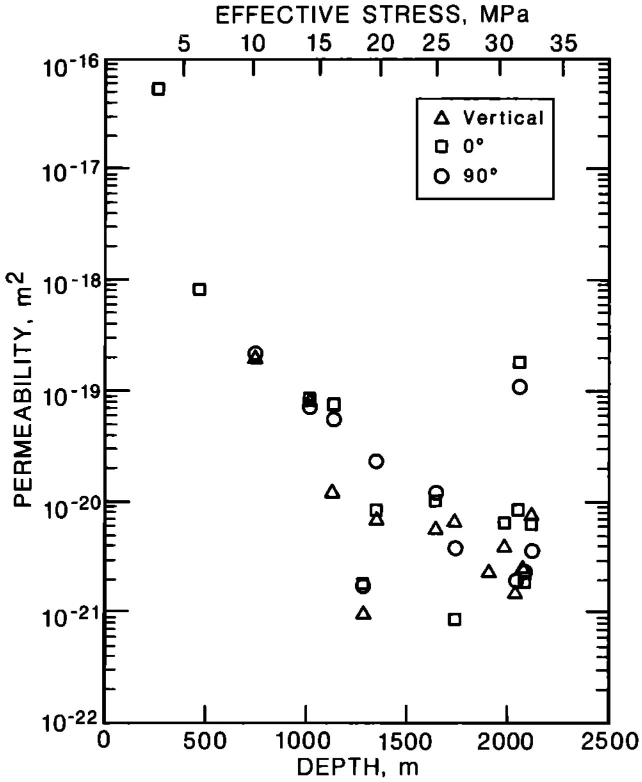

Figure 2. Permeability of unfractured Cajon Pass cores as a function of depth and effective pressure (P_c-P_p). Depth does not scale directly with pressure because the rock densities vary, particularly between the sandstones (<500 m) and the crystalline rocks (>500 m). $10^{-21}m^2$ = 1 nanodarcy.

The permeabilities of the two sandstones reflect a difference in texture as much as effective pressure. Permeabilities were $5.4 \times 10^{-17}m^2$ at 272 m (σ_e = 3.4 MPa) and $8.3 \times 10^{-19}m^2$ at 480 m (σ_e = 6.1 MPa). Although we expect the flow to be lower at greater effective pressures, the large difference is surprising considering the extremely porous and friable nature of the deeper sample. This is probably a result of the more abundant void-filling clay particles in the 480 m sample compared to the cleaner, better sorted rock at 272 m. Clay minerals have extremely low permeabilities under pressure (10^{-18} to $10^{-21}m^2$), and are effective in reducing the permeability of clay-rich sandstones (Morrow et al., 1984).

Permeability is plotted as a function of depth and effective pressure for both the sandstones and crystalline samples in Figure 2. Note that stress does not scale directly with depth in this plot, due to the lower density of the sandstone layer, and the small variations in density between the various deeper rocks. For the crystalline rocks between 500 and 2100 m, permeability decreased sharply with depth due to the progressive closure of cracks at the higher pressures. This trend is quite striking because permeability decreased more rapidly with applied pressure for the Cajon Pass samples than for other well studied crystalline rocks such as Westerly, Barre or Chelmsford Granites (see for example, Brace et al., 1968). These latter rocks all have permeabilities of around 10^{-18} to $10^{-19}m^2$ at low pressures like the Cajon Pass samples, but they do not reach permeability values of $10^{-21}m^2$ until several hundred MPa effective pressure has been applied. The Cajon Pass rocks, on the other hand, have permeabilities of around $10^{-21}m^2$ at only 20 to 30 MPa effective pressure, an order of magnitude lower stress. We can conclude, therefore, that the Cajon Pass rocks are exceptionally tight compared to the expected values based on previous studies of crystalline rocks.

Many of the samples exhibit a strong foliation in hand specimen that would suggest significant flow anisotropy. However, examination of Table 1 shows that, with a few exceptions, the anisotropy for such rocks was generally around a factor of 2. This anisotropy does not result in a scatter of the data that is so great as to obscure the general trend of permeability with depth. The highest permeability for these samples was often in a horizontal direction (along the bedding), but because many of the rocks are also folded, this relation does not always apply. For the deepest rocks, stress relief cracking may be important. This possibility will need further study.

Petrographic Observations

A few of the samples do not follow the permeability trend shown in Figure 2. Such rocks might indicate horizons that could be local barriers to flow such as the tight banded gneiss at 1284 m or regions of enhanced flow such as the granodiorite at 2056 m. These and other samples were examined in thin section to determine what might cause the anomalous behavior of certain rocks, and why the permeabilities are generally low. Petrographic observations show extensive evidence of crack healing and sealing at all depths, indicating that the circulation of hydrothermal fluids has played a significant role in reducing the permeability of the rocks.

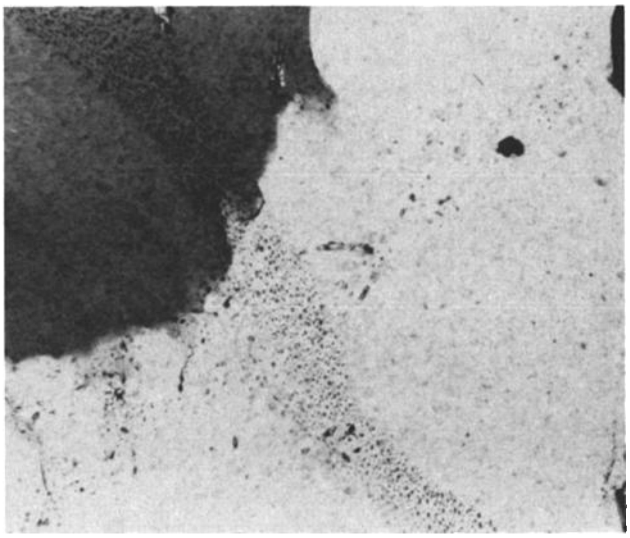

Figure 3. Photomicrograph of a quartzose gneiss, 1284 m (90°). Image is 0.9 mm across. A healed crack (string of isolated bubbles) cuts across two quartz grains.

An example of nearly complete crack healing in the quartzose gneiss is shown in Figure 3, (1284 m, 90°, $k=1.9 \times 10^{-21} m^2$) where a plane of fluid inclusions marks the former position of an intergranular crack. Note that the boundary between the two quartz grains (different shades of grey) is closed and free of alteration minerals that could provide an intergranular flow path. Quartz has been found to be an effective crack-sealing mineral when subjected to fluid flow under low temperature conditions (Morrow et al., 1985). This probably accounts for the anomalously low permeability of the nearly monomineralic-quartz gneiss compared to the other, more mafic rocks. Grain boundaries sealed by other minerals such as calcite or zeolites are also common in the low permeability diorites and hornblende diorites (1741 m, 2042 m), even though the interiors of the grains may be cracked or altered. In contrast, the granodiorite at 2056 m, (0°, $k=1.9 \times 10^{-19} m^2$) shows that extensive parallel and unhealed fractures are the cause of the untypically high permeability and flow anisotropy.

Discussion

The very low permeability measurements from the first phase of the Cajon Pass drilling program have been most unexpected. However, it would be unwise to extrapolate the strong decrease in permeability to greater depths. Rocks from the second phase of drilling will be most interesting in completing the permeability versus depth picture.

How do these laboratory measurements relate to the in situ environment? Our measurements represent a lower limit to permeability as they do not include the contributions of larger scale fractures and joints. However, the low values are similarly reflected in the in situ bulk permeability, as the downhole studies at Cajon Pass have shown. Coyle and Zoback (1987) report in situ permeability at the 2000 m level of around $2 \times 10^{-18} m^2$, which is surprisingly low for rocks that contain natural fractures. They attribute the low permeability to extensive joint filling by such minerals as chlorite and various zeolites, which are readily visible along the length of the core. This appears to be a larger-scale expression of the crack healing and filling that we observed under the microscope, suggesting that hydrothermal fluids active in the past have affected permeability on all scales. The in situ tests also show that the pore pressure is only a few percent above hydrostatic at this location, possibly a result of local topography. This may not reflect the conditions within the fault, however, and only further drilling within the fault zone itself will answer that question. In any case, both the laboratory and in situ data at Cajon Pass indicate that at one time hydrothermal circulation was extensive, but that now the circulation of fluids in the vicinity of the fault may be inhibited due to the extremely tight nature of the rocks.

Acknowledgement. This research was supported by the USGS under the Deep Continental Studies Program.

References

Brace, W.F., Walsh, J.B. and Frangos, W.T., Permeability of granite under high pressure, J. Geophys. Res., 73, 2225, 1968.

Brace, W.F. and Kohlstedt, D.L., Limits on lithospheric stress imposed by laboratory experiments, J. Geophys. Res., 85(B11), 6248, 1980.

Coyle, B.J. and Zoback, M.D., In situ permeability and pore pressure measurements in the Cajon Pass drillhole, EOS, 68, 1490, 1987.

Lachenbruch, A.H., and Sass, J.H., Heat flow and energetics of the San Andreas fault zone, J. Geophys. Res., 85(11), 6185, 1980.

Morrow, C.A., Shi, L.Q. and Byerlee, J.D., Permeability of fault gouge under confining pressure and shear stress, J. Geophys. Res., 89, 3193, 1984.

Morrow, C.A., Moore, D.E. and Byerlee, J.D., Permeability changes in crystalline rocks due to temperature: effects of mineral assemblage, Mat. Res. Soc. Symp. Proc., 44, 467, 1985.

O'Neil, J.R. and Hanks, T.C., Geochemical evidence for water-rock interaction along the San Andreas and Garlock faults of California, Jour. Geophys. Res., 85(B11), 6286, 1980.

Pezard, P.A., Luthi, S.N., Anderson, R.N. and Ollier, G.R., Fracture characterization from continuous electrical measurements in the basement of the Cajon Pass DOSECC drillhole, California, EOS, 68, 1495, 1987.

C. Morrow and J. Byerlee, U.S. Geological Survey, Menlo Park, California 94025.

(Received February 11, 1988;
revised June 6, 1988;
accepted June 7, 1988)